ELSEVIER

Coastal Engineering 47 (2002) 211–235

Coastal Engineering
An International Journal for Coastal, Harbour and Offshore Engineers

www.elsevier.com/locate/coastaleng

Variability of shore and shoreline evolution

Marcel J.F. Stive[a,*], Stefan G.J. Aarninkhof[a], Luc Hamm[b], Hans Hanson[c], Magnus Larson[c], Kathelijne M. Wijnberg[d], Robert J. Nicholls[e], Michele Capobianco[f]

[a] *Delft University of Technology and Delft Hydraulics, Delft, The Netherlands*
[b] *Sogreah, Grenoble, France*
[c] *University of Lund, Lund, Sweden*
[d] *IMAU, University of Utrecht, Utrecht, The Netherlands*
[e] *Flood Hazard Research Centre, Middlesex University, Enfield, UK*
[f] *SATE–Systems and Advanced Technologies Engineering S.r.L., Venice, Italy*

Abstract

Shore and shoreline evolution both due to natural and human-induced causes or factors can be variable over a wide range of different temporal and/or spatial scales. Our capability to understand and especially predict this variability is still limited. This can lead to misinterpretation of coastal change information, which hampers informed decision making and the subsequent design and implementation of (soft) engineering interventions. Collecting and describing example observations of shore and shoreline variability is one way to support and improve such human intervention. This paper describes causes and factors for the variability and the resulting possible evolutions of wave-dominated shores and shorelines, which are illustrated by a number of case studies. The new element of this work is that the variability is described in terms of a range of different time and space scales, which helps to structure such analysis. However, it is difficult to generalise the results for arbitrary situations, especially on decadal time scales. Scientific and engineering improvements require more quantitative insight into the physical mechanisms behind the free and forced shore behaviour responsible for the variability.

Keywords: Variability; Shore evolution; Shoreline evolution

1. Introduction

The objective of this paper is to provide a quantitative insight into the 'autonomous' variability of the shore, in general, and the shoreline, in particular, in the context of shore nourishment design. Autonomous refers to the behaviour of the shore(-line) in the absence of an intended engineering intervention. When considering a nourishment intervention, it is essential to understand the temporal and spatial variability of the shore, in order (1) not to "fall in the trap" of nourishing a coast which would accrete anyway, or, more generally, (2) not to under- or overnourish a coast which exhibits oscillatory behaviour. These arguments deal with the success and efficiency of nourishment interventions. Here, we do not explicitly address the question of the impact of the nourishment on the after-project shore variability. Instead, we refer to the paper of Capobianco et al. (2002).

Efforts have been undertaken in the literature to quantify shoreline variability. A particular form of this

* Corresponding author.
E-mail address: m.j.f.stive@ct.tudelft.nl (M.J.F. Stive).

0378-3839/02/$ - see front matter © 2002 Elsevier Science B.V. All rights reserved.
PII: S0378-3839(02)00126-6

variability is 'beach mobility', which was defined by Dolan et al. (1978) as the standard deviation of the shoreline relative to its linear trend. It has been suggested that this is a function of the morphodynamic state of the beach (Short and Hesp, 1982): dissipative, intermediate, and reflective beaches correspond to low–moderate, moderate–high, and low beach mobility, respectively. On Australian beaches, the standard deviation of the shoreline position measured several times every year ranges between 5 and 14 m when temporal data series of 1 to 5 years are considered. More moderate values are found in three 12–14-year data sets discussed further on, viz. 7 to 8 m for two Japanese sites and 2 to 3 m for Duck (USA). In contrast, the shoreline mobility of the Holland coast (characterised as dissipative) during the period 1964–1992 (represented by the position of +1 m NAP ≈ MSL contour yearly measured) is higher, about 20 m (Guillén et al., 1999), which might imply that the beach mobility parameter increases with time scale.

A specifically interesting phenomenon is the existence of spatial fluctuations in the position of the shoreline, with periodicities that are irregular to quasi-sinusoidal in form (known since Evans, 1939), which have been found to often be moving along the shoreline. These propagating features cause the shoreline to fluctuate at decadal time and associated space scales, which are particularly relevant in the present context.

As we will indicate, there exists a variety of periodicities and associated length and space scales in the observations. Besides extending the data set with more observational examples, the present paper aims to contribute to this topic by providing an inventory of shoreline variability on different scales. Furthermore, it should be stressed that shoreline variability is only one index of the behaviour of the entire shoreface. Understanding both the shoreline and the more integrated shore (i.e., shoreface-body) behaviour is relevant for efficient nourishment management purposes.

2. Shore and shoreline variability on different scales

Temporal shoreline variability may easily be observed by plotting a particular shoreline position against time. Two examples of this from the Netherlands are given in Fig. 1a and b, illustrating autonomous shoreline evolution (the Wadden Sea barrier island Schiermonnikoog) and human-influenced evolution (the Zeeland barrier island of Goeree), respectively. Three shoreline indicators, measured at yearly intervals, are used (1) low water (LW), (2) high water (HW) and (3) the dunefoot. As these figures indicate, temporal variations on different scales may be discerned. On the centennial scale, the shoreline shows a clear trend of shore advance and shore retreat, respectively. Note that the centennial trends of the LW, HW and duneface position are not necessarily the same. On the decadal scale, the LW and HW shorelines of Schiermonnikoog show a clear oscillation, associated with 'sand waves' induced by coastal inlet channel migration cycles. Note that this is not reflected in the dunefoot behaviour. One such natural oscillation is also apparent in the Goeree shoreline, which in contrast is also reflected in the dunefoot. The construction of the Brouwersdam closing off the coastal inlet to its south causes a perturbation of the trend. Generally, we may observe that shorter, annual variations of the LW line are strongest and of the dunefoot the weakest.

The examples in Fig. 1 indicate that the variability of shorelines displays itself differently in space and in time and differently at the LW, HW, and dunefoot position. By looking more closely at the causes and effects illustrated by case examples in the following discussion, we may try to understand and thereby quantify the shoreline variability more precisely. As an introduction, Table 1a and Table 1b list, respectively, natural and human causes and factors and the resulting typical coastal evolution trends by scale. This four-part scale division rests upon the idea that coastal morphodynamic processes can be partitioned into 'naturally occurring' levels at similar time and space scales, and each level interacts with higher and lower levels in a systematic manner (Capobianco et al., 1998). Each level in the hierarchy or cascade sees the larger-scale levels as constraints and/or boundary conditions and the smaller-scale levels as representing the internal behaviour.

While, in principle, all, or almost all, typical evolutions may be associated with the causes and factors behind shore evolution, we have ordered the causes and the evolutions approximately by importance, following Stive et al. (1990). Note that for the

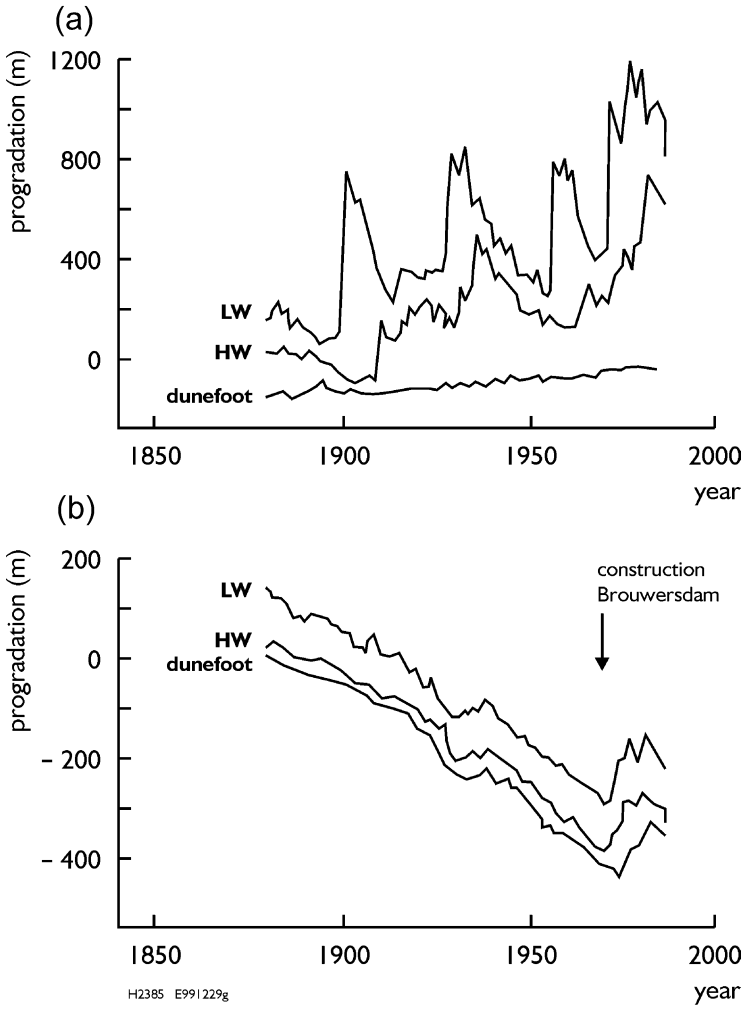

Fig. 1. Evolution of the mean LW, HW (based on tide records) and dunefoot shoreline since 1880. (a) Northwest location of Schiermonnikoog. (b) West location of Goeree (The Netherlands).

evolutions associated with natural causes and factors, the typical evolutions are trends for the larger-scale and for the smaller-scale fluctuations. For the evolutions associated with human causes, these are trends and trend changes, respectively.

However, we would wish to state that generally speaking, the notion of relative importance might be difficult to justify. Dominance will vary from coastal section to coastal section. For instance, in Britain, a major long-term interference is sediment starvation due to cliff protection, which in Table 1b would fall under coastal structures and/or coastal management. Also, note that there is no unique process behind each cause. For instance, river regulation can be, but is not necessarily, the same problem as sediment starvation.

We remark that not all typical evolutions are discussed in the indicated subsections. The emphasis in most cases is on ‘natural’ variability. Consequently, there is little reference to trend changes that involve damping and asymptotic behaviour, which are often encountered in cases of human intervention. A typical response in the case of shore nourishment of an unconstrained coast may be damping of the perturbation, which also displays itself as asymptotic behaviour, viz. in the evolution of the integrated excess volume. A clear case of asymptotic behaviour may occur updrift of

Table 1a
Natural causes and factors and associated evolutions for shore and shoreline variability; see text for further explanation (based upon and adapted from Stolk, 1989 and Stive et al., 1990)

Scale	Natural causes/factors	Typical evolutions	Subsection in this paper
Very long term (time scale: centuries to millenia; space scale: ~ 100 km and more)	⇒ 'sediment availability' ⇒ relative sea-level changes ⇒ differential bottom changes ⇒ geological setting ⇒ long-term climate changes ⇒ paleomorphology (inherited morphology)	⇒ (quasi-)linear trends ⇒ trend changes (reversal, asymptotic, damping) ⇒ fluctuations (from (quasi-) cyclic to noncyclic	Late Holocene Variability
Long term (time scale: decades to centuries; space scale: ~ 10–100 km	⇒ relative sea-level changes ⇒ regional climate variations ⇒ coastal inlet cycles ⇒ 'sand waves' ⇒ extreme events	⇒ (quasi-)linear trends ⇒ fluctuations (from (quasi-) cyclic to noncyclic) ⇒ trend changes (reversal, asymptotic, damping)	Intercentennial variability
Middle term (time scale: years to decades; space scale: ~ 1–5 km)	⇒ wave climate variations ⇒ surf zone bar cycles ⇒ extreme events	⇒ fluctuations (from (quasi-) cyclic to noncyclic) ⇒ (quasi-)linear trends ⇒ trend changes (reversal, asymptotic, damping)	(Inter-)annual and (inter-) decadal variability
Short term (time scale: hours to years; space scale: ~ 10 m–1 km)	⇒ wave, tide and surge conditions ⇒ seasonal climate variations	⇒ fluctuations (from (quasi-) cyclic to noncyclic) ⇒ (quasi-)linear trends ⇒ trend changes (reversal, asymptotic, damping)	(Inter-)seasonal and (inter-) annual variability

a longshore interrupting structure, where the coastline orientation can reach a new equilibrium.

In the following sections, we present and discuss a number of case examples at the various scales, starting with the smallest time and space scales that we consider relevant for coastal management.

3. Observations of shore and shoreline variability

3.1. Seasonal and interseasonal shore variability

Beach variability on the seasonal and interseasonal time scale is the shortest-term type of variability relevant to coastal management. It concerns periodic fluctuations in the dynamic behaviour of a beach on the time scales of seasons down to single events. An example of the first is the systematic variation of a beach with the seasons. Classically, there is a relatively steep 'swell' profile during the summer when incoming waves are mild and a lower slope 'storm' profile during the winter when high-energetic wave conditions can occur (Komar, 1998). On the event time scale, and in correspondence with the seasonal variability, we may observe rapid shoreline erosional events during storms, alternating with periods of slower, but near continuous accretion of new beach-front when wave conditions are mild. This seasonality, however, is not universal due to regional and/or temporal interseasonal variations in wave climate.

The case of the Rhône delta coast (France) in the Mediterranean Sea is an example where seasonal variations are observed, which are not in accordance with the classic picture. Fig. 2a shows the evolution of the shoreline (defined at the mean sea level) over 10 years at one typical location of La Gracieuse beach located about 7 km northeast of the Rhône mouth (Moulis et al., 1999). The shoreline of this dissipative beach is stable as shown by the linear trend given in the figure; its beach mobility index is 13.2 m. Seaward movements of the shoreline in summer and shoreward movements in winter are observed. The peculiar aspect of these fluctuations is that sand is accumulated in front of the dune by winter storms and redistributed seawards by strong offshore winds (the so-called Mistral) in spring and summer as shown in Fig. 2b.

Table 1b
Some typical human-induced causes and factors and associated evolutions for shore and shoreline variability: see text for further explanation (based upon and adapted from Stolk, 1989 and Stive et al., 1990)

Scale	Human causes/factors	Typical evolutions	Subsection in this paper
Very long term (time scale: centuries to millenia; space scale: ~ 100 km and more)	⇒ human-induced climate change ⇒ major river regulation ⇒ major coastal structures ⇒ major reclamations and closures ⇒ structural coastal (non)management	⇒ (quasi-)linear trends ⇒ trend changes (reversal, asymptotic, damping) ⇒ fluctuations (from (quasi-)cyclic to noncyclic)	Late Holocene Variability
Long term (time scale: decades to centuries; space scale: ~ 10–100 km	⇒ river regulation ⇒ coastal structures ⇒ reclamations and closures ⇒ coastal (non)management ⇒ natural resource extraction (subsidence)	⇒ trend changes (reversal, asymptotic, damping) ⇒ (quasi-)linear trends ⇒ fluctuations (from (quasi-)cyclic to noncyclic)	Intercentennial variability
Middle term (time scale: years to decades; space scale: ~ 1–5 km)	⇒ surf zone structures ⇒ shore nourishments	⇒ trend changes (reversal, asymptotic, damping) ⇒ fluctuations (from (quasi-) cyclic to noncyclic)	(Inter-)annual and (inter-) decadal variability
Short term (time scale: hours to years; space scale: ~ 10 m–1 km)	⇒ surf zone structures ⇒ shore nourishments	⇒ trend changes (reversal, asymptotic, damping) ⇒ fluctuations (from (quasi-)cyclic to noncyclic)	(Inter-)seasonal and (inter-) annual variability

Note that while very long-term human effects are being observed (e.g., the growth of the Ebro delta due to deforestation), they largely remain a theoretical concept.

The above descriptions indicate a coupling between the instantaneous conditions and the shore response. The first effort to classify beach morphology as a function of one (or more) instantaneous dimensionless parameters stems from Wright and Short (1984). Based on an extensive data set of field observations along the Australian coast, Wright and Short identify six distinctive 'beach states' that vary between the extreme states 'dissipative' (State A) and 'reflective' (State F). The four intermediate states comprise the so-called Longshore Bar Trough (LBT), Rhythmic Bar and Beach (RBB), Transverse Bar and Rip (TBR), and Low-Tide Terrace (LTT). Wright and Short (1984) relate the beach state to a dimensionless fall velocity parameter, $\Omega = H_b/(w_s T)$, which covers characteristics of both the sediment (via the fall velocity, w_s) and the wave climate (via the wave period, T, and the breaking wave height, H_b). Reflective beach states are found for $\Omega < 1$, dissipative states for $\Omega > 6$. Wright et al. (1986) recognise that a current beach state not only depends on time-dependent forcing conditions but also on preceding states; hence, they apply a weighted, running mean of Ω. Masselink and Short (1993) extended the Wright and Short model for application to mesotidal and macrotidal beaches. Their extended classification is based on Ω and an additional parameter, the relative tide range (RTR), defined as the ratio of the mean spring tide range (MSR) and the breaker height (H_b). The relative tide range reflects the relative importance of swash, surf zone, and shoaling wave processes. On beaches with a large tidal range, bars are less likely to be developed.

The above beach state classification models are based on equilibrium concepts in the sense that they

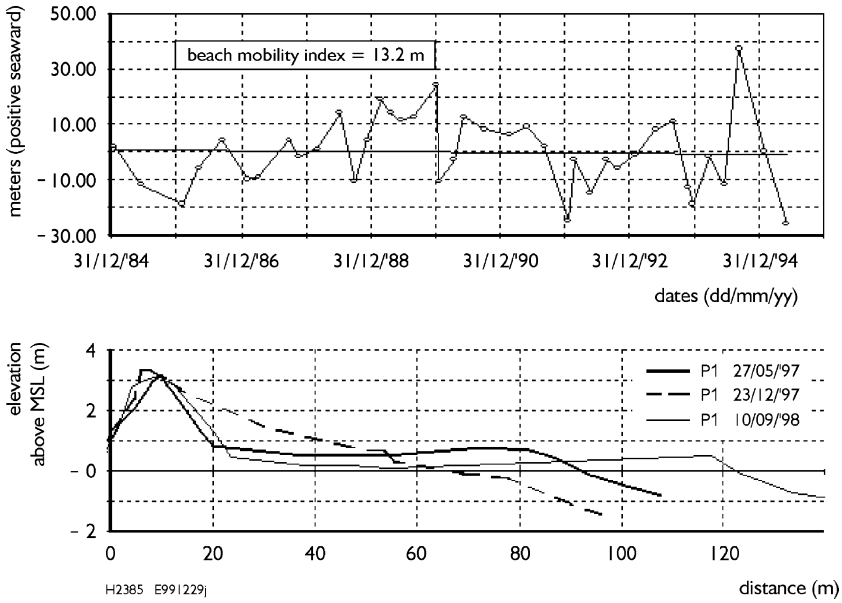

Fig. 2. Seasonal shoreline and beach profile evolution at La Gracieuse beach (France).

describe morphological states as a function of forcing parameters. Lippmann and Holman (1990), who also addressed the dynamics of the system by paying attention to the transition between different states, extended the concept based on time-averaged video observations of the surf zone at Duck over 2 years. Lippmann and Holman present an eight-state model of sand bar morphology which is essentially the same as Wright and Short's six-state concept, except that they further divide the LBT state and the TBR state to better define longshore variability in bar morphology. Higher states are associated with dissipative conditions and vice versa. Upstate transitions represent seaward migration of the bars and are observed with time scales of change of the incident wave energy. It could not be concluded whether they occur sequentially. Downstate transitions, on the other hand, coincide with lower wave conditions, thus representing accretional progression. Downstate transitions occur sequentially and their time scale considerably exceeds the time scale of change of the incident wave energy; hence, the downstate migrating bar system tends to depend more heavily on its previous configuration.

With the help of the concept of morphologic states, the seasonal and interseasonal variability of beaches (or 'beach mobility') can be assessed, though only qualitatively. Obviously, beach mobility increases with increasing temporal variability of the beach states observed. However, considerable change in the absolute profile evolution can also occur without the *state* changing (Wright and Short, 1984), in particular, in case of the intermediate states. Hence, to quantify beach mobility in more detail, different methods need to be deployed. Two suggestions will shortly be treated here.

One method concerns the analysis of detailed field measurements of one single element of a coastal system that easily allows for quantification while being representative for the morphodynamic behaviour of the overall system at the same time. A vertically referenced waterline is a good candidate. Fig. 3 (after List and Farris, 1999) shows field surveys of some 80 km of shoreline along the East Coast of the USA, around the US Army Engineer Field Research Facility in Duck, NC. The lower half of the upper panel indicates shoreline changes during a period of erosion (October 13–20), while shoreline accretion during the subsequent period of calm wave conditions (October 20–25) is given in the upper half. As can be observed, absolute changes on the event

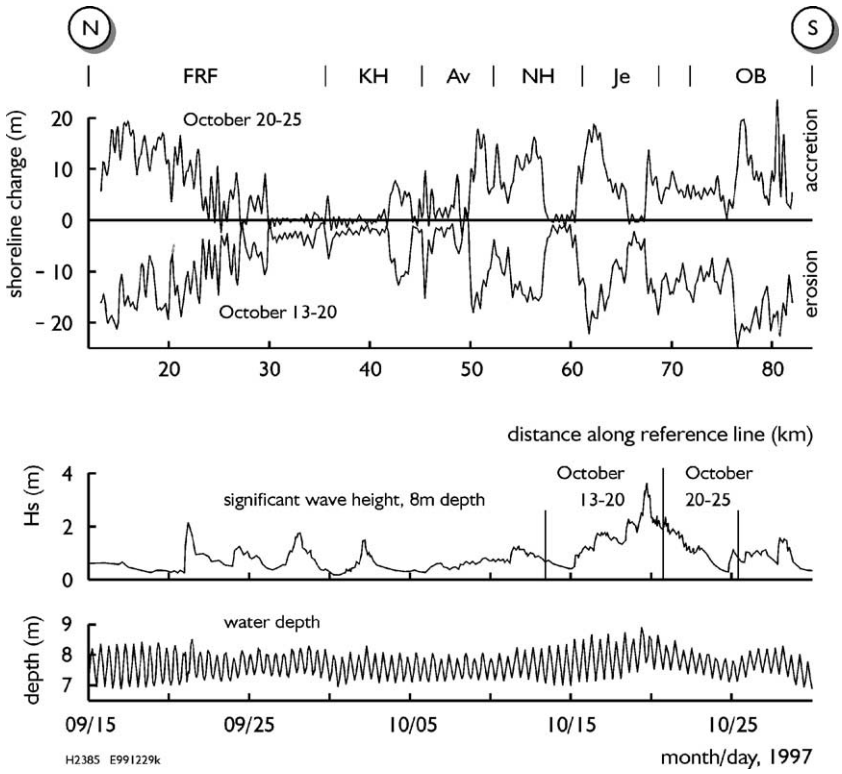

Fig. 3. Field observations of erosion (13–20 October 1997) and accretion (20–25 October 1997) along the coast of North Carolina in response to a storm on 19 October 1997. FRF indicates the US Army Corps of Engineers Field Research Facility, Duck (after List and Farris, 1999).

time scale amount up to 20 m. But more importantly, changes turn out to be almost fully reversible along the entire coastline. This is thus a near-perfect example of a periodic storm–fair weather cycle. This yields valuable information on the autonomous shoreline variability of these beaches, suitable for both scientific analysis and management practice.

Another approach is to quantify shoreline variability from ARGUS video observations of the nearshore zone. ARGUS video data are collected on an hourly base, hence allowing for an accurate assessment of shoreline changes on the seasonal and event time scale. An example of such an application is given below. Fig. 4 (courtesy Sallenger (USGS)) shows a so-called time stack image of a nourished beach at St. Petersburg (USA), which was obtained by accumulating time-averaged image intensities sampled at subsequent days along a fixed cross-shore array. Time is given vertically, while the horizontal axis gives the cross-shore distance, with deeper water at the right-hand side of the image and the dry beach at the left-hand side. The bright intensity band that diagonally crosses the image (say from $x = 70$ m in January 1997 to $x = -5$ m in April 1998) indicates the location of the shoreline break, which behaviour reflects shoreline changes (Plant and Holman, 1997). As can be seen from Fig. 4, an erosional trend occurs over the full monitoring period (about 75 m after 15 months). However, during summer, the shoreline is approximately stable, which reflects a seasonal variability in the morphodynamic adjustment (or behaviour) of this beach after nourishment.

As illustrated by the previous examples, variability in shoreline position may occur due to cross-shore displacements of material induced by temporal variation in the wave conditions (seasonal, storm–fair weather cycle). However, longshore mobility of spatial patterns in shoreline position may also con-

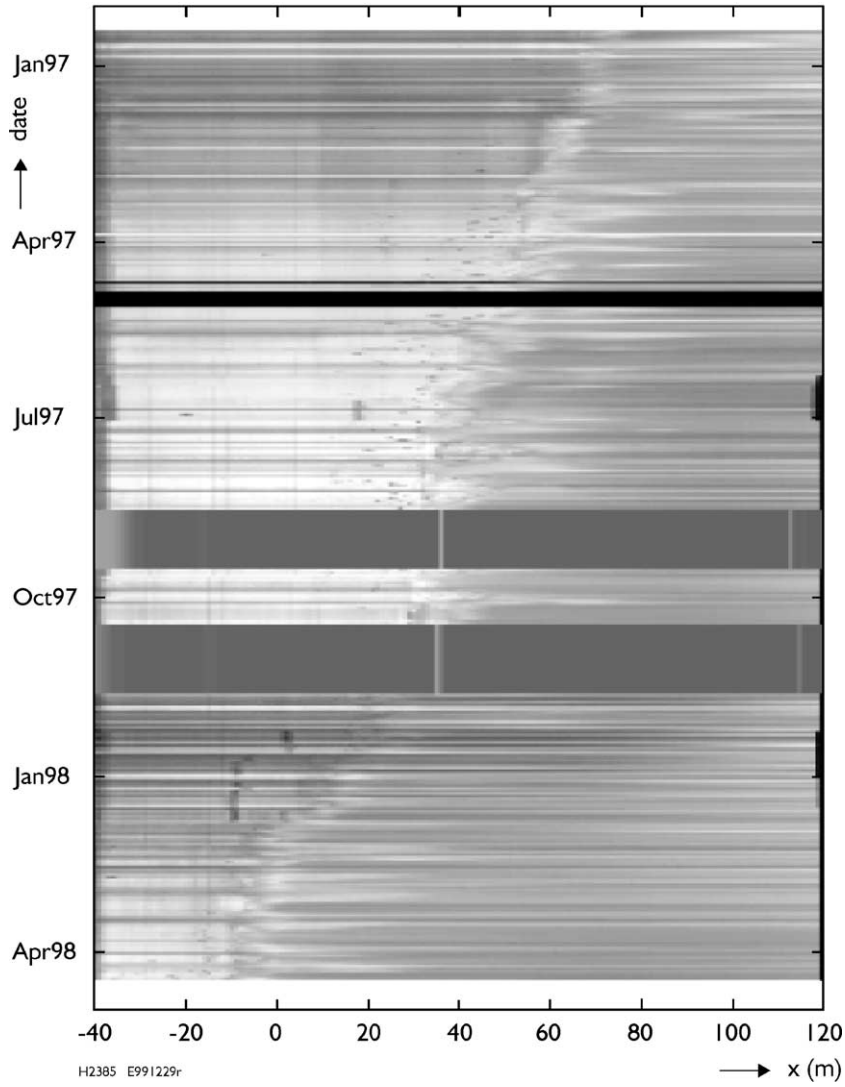

Fig. 4. Nourishment evolution St. Petersburg, FL, USA; see text for explanation (courtesy Sallenger).

tribute to cross-shore shoreline mobility. This is not only relevant on the interannual time scale, as is shown later in the subsection on Interdecadal Shoreline Variability, but also on shorter time scales. This is illustrated by shoreline data obtained from the ARGUS video time-exposure data set collected at Egmond (The Netherlands). Over an 81/2-month period, the position of the spring high-tide waterline (approximating the +1-m contour) was extracted over a 3.5-km stretch of coastline (Fig. 5a). The position was measured relative to the longshore axis (shore parallel) of a local coordinate system. It appears that a relatively stable, large-scale pattern in shoreline position is present, which is obviously related to the interannual shoreline evolution pattern shown in Fig. 9. Applying an EOF analysis to this data set reveals that deviations from the time-averaged shoreline position consist for about 40% of variations in the cross-shore amplitude of the large-scale shoreline pattern (described by first EOF). Sixty percent of the variation, however, consists of smaller-scale perturbations of the shoreline config-

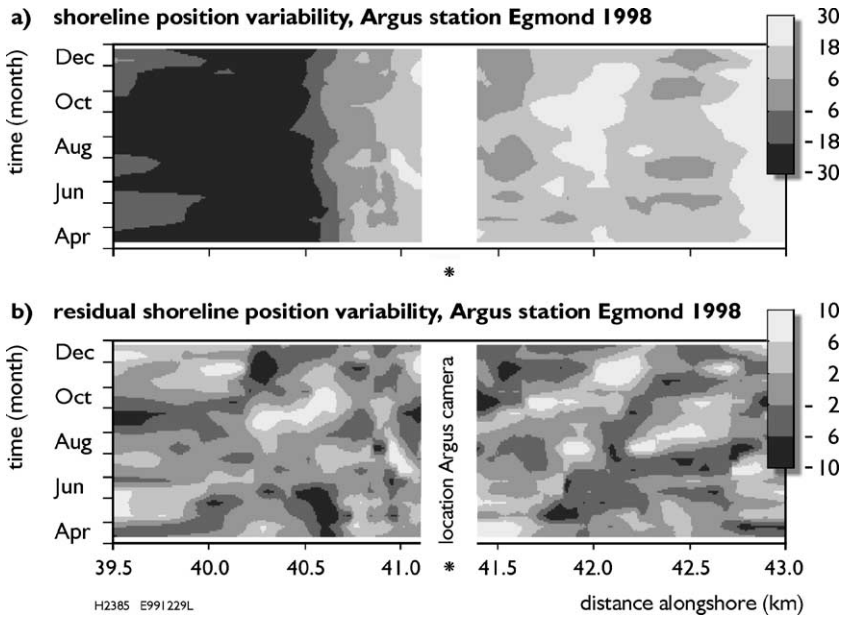

Fig. 5. Interannual shoreline evolution near Egmond aan Zee (The Netherlands). (a) Shoreline position derived from Argus time-exposure images at spring high tide (position corrected for variations in tidal elevation). Gray scales indicate the deviations (m) from the time- and space-averaged shoreline position. (b) Residual shoreline variation, uncorrelated with large-scale shoreline pattern (based on EOF analysis); panel b follows panel a when the shoreline position variation described by the first EOF is removed. Gray scales indicate the magnitude of these residual deviations (m).

uration, some of which propagate alongshore (Fig. 5b).

3.2. (Inter-)annual variability

In order to illustrate the typical variability in shoreline position on the interannual scale, results from the analysis of three high-quality data sets are discussed here. One data set originates from the US Army Engineer Field Research Facility in Duck, NC, where profile surveying has been carried out approximately biweekly since 1981 (Howd and Birkemeier, 1987; Lee and Birkemeier, 1993; Birkemeier et al., 1999). The two other data sets are from Japan, one collected at Ogata on the Japan Sea coast (Tsuchiya et al., 1994) and the other at Ajigaura on the Pacific Ocean coast (Uda et al., 1990). In the Japanese data sets, surveying of the beach profiles was done on a weekly basis from the early 1970s. The three data sets encompass 12 to 14 years of measurements, giving a good basis for determining typical changes at the interannual scale as well as seasonal variability. Furthermore, since the temporal resolution was at the weekly scale, the effects of storm events could be assessed to a large extent. All measurements discussed here refer to the local mean sea level and the values shown are deviations from the mean shoreline location based on the time series.

Fig. 6.1a, 6.2a, and 6.3a displays the time series of shoreline position recorded at Duck, Ogata, and Ajigaura, respectively. The overall trends over the measurement periods for the three sites are quite different, where slight accretion is observed at Duck, marked erosion at Ogata, and almost no net movement at Ajigaura. Also, the variability of the signals is quite different at the three sites with the largest fluctuations at Ajigaura and the smallest at Duck. Using the measured time series directly, the calculated standard deviation was 7.9, 7.7, and 2.3 m for Ajigaura, Ogata, and Duck, respectively. However, after removing the trends in the data series, the standard deviation was significantly reduced for the two latter series (to 2.6 and 1.3 m, respectively), whereas the value calculated for the Ajigaura series was less affected (6.2 m). Singular spectrum analysis (SSA; Vautard et al., 1992; Rózynski et al., 2001) was employed to remove

the long-term (i.e., decadal) trends in the data series (see Southgate et al., 2002). SSA is a data-adaptive technique that is powerful for detrending short, noisy time series such as the ones analysed here. Fig. 6.1a, 6.2a, and 6.3a also includes the trends identified in the different time series utilising SSA.

After employing SSA to extract the long-term trends in the shoreline evolution, spectral analysis was applied to determine the oscillatory characteristics of the signals. Thus, the power content in the low-frequency components was removed without markedly affecting the distribution of the power at

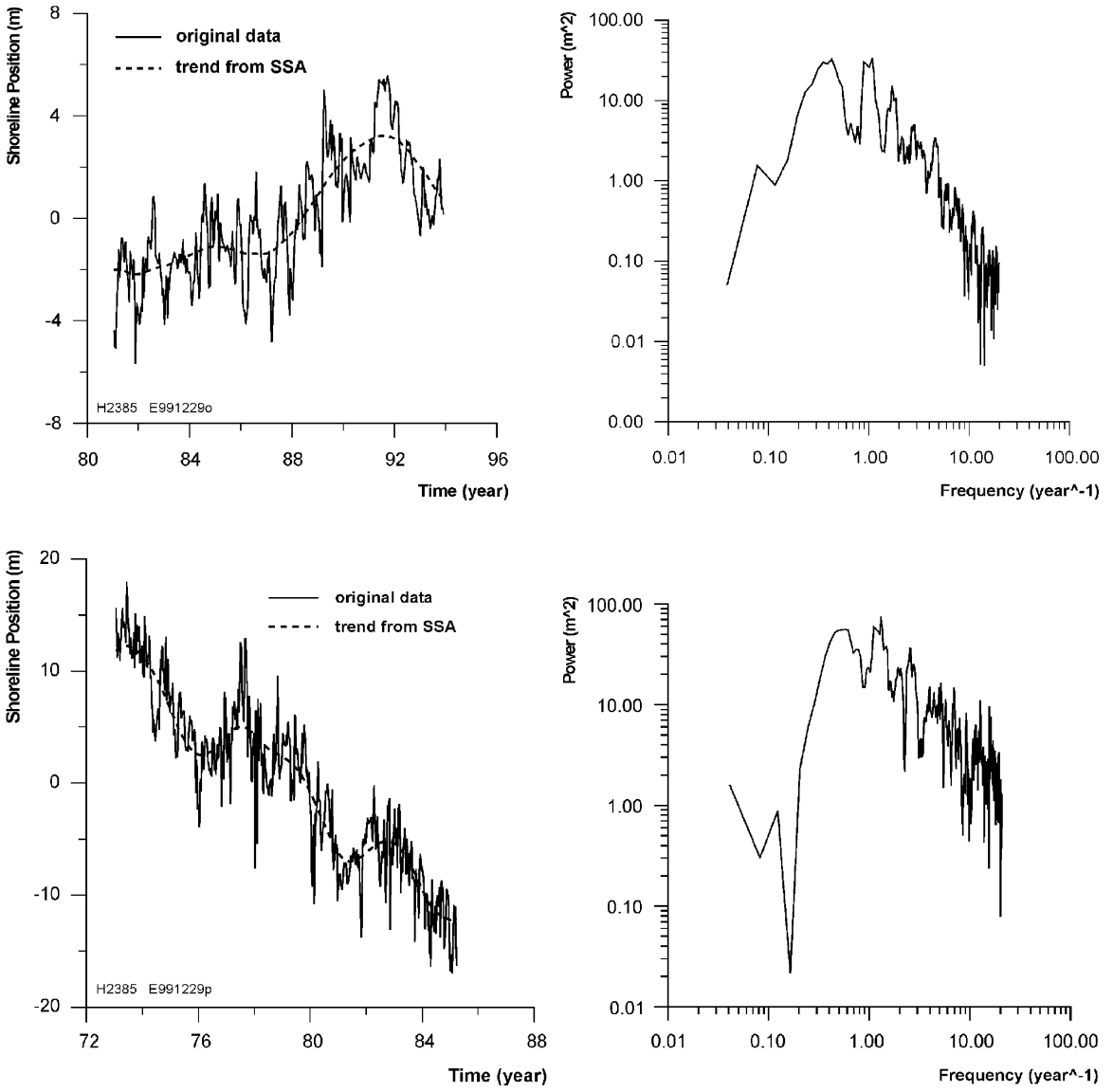

Fig. 6. 1: (left) Time series of measured shoreline position at Duck, North Carolina; and (right) calculated spectrum of the shoreline position after trend removal. 2: (left) Time series of measured shoreline position at Ogata, Japan; and (right) calculated spectrum of the shoreline position after trend removal. 3: (left) Time series of measured shoreline position at Ajigaura, Japan; and (right) calculated spectrum of the shoreline position after trend removal.

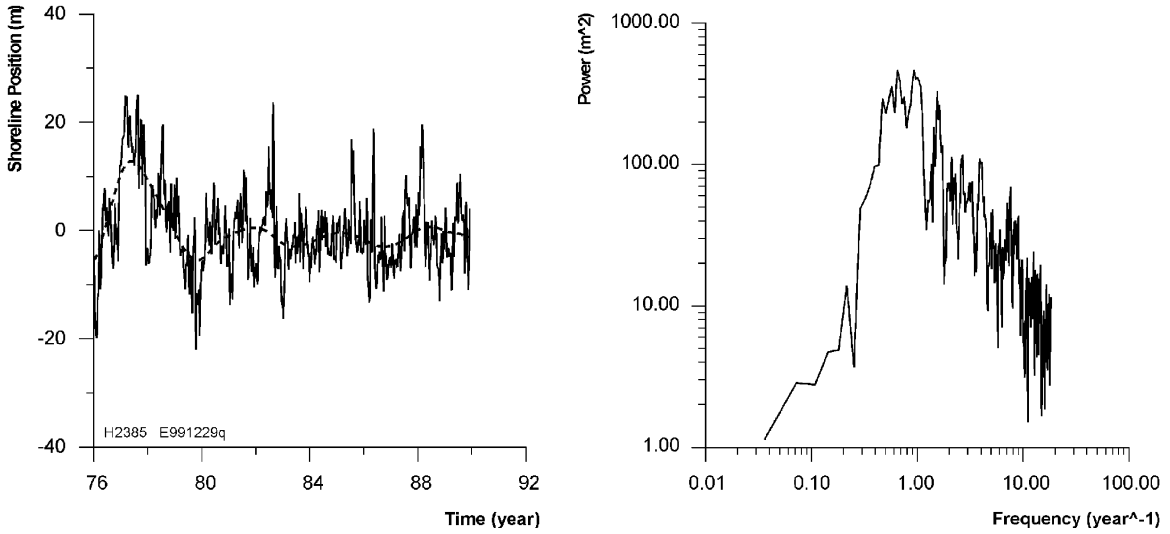

Fig. 6 (*continued*).

higher frequencies (spectral analysis with and without trend removal was performed to confirm this as well as the location of peaks in the higher frequency part of the spectrum). The multitaper method (MTM) of spectral analysis was applied to the derived data sets (Thomson, 1982). MTM is a nonparametric spectral analysis method, i.e., it does not prescribe an a priori statistical model (e.g., autoregressive model) for the physical process generating the time series under analysis, and it has been widely used in analyzing time series of geophysical data. The method is suitable for time series, which is believed to exhibit a spectrum containing both continuous and singular components (Dettinger et al., 1995). Figs. 6.1b, 6.2b, and 6.3b illustrates the spectra calculated for the Duck, Ogata, and Ajigaura data, respectively, after the trends were removed. The magnitude of the characteristic shoreline fluctuations is reflected in the calculated power of the signal, yielding the highest values for Ajigaura followed by Ogata and Duck. This magnitude may be related to the variability in the wave climate including the absolute magnitude of the most severe storms. However, the grain-size characteristics are also of significance for the shoreline response.

All spectra show a pronounced peak corresponding to a 1-year cycle indicating the effects of seasonal exchange of material across the profiles (for the Ogata data, however, the centre of the peak is displaced towards a period somewhat shorter than 1 year). Several higher frequencies may be observed in the data sets, probably associated with the typical return period of different storm events. Another characteristic feature of the spectra is the rate at which the power decreases at higher frequencies. Again, this rate reflects the wave climate at the specific site and how the storm characteristics (magnitude, return period, and chronology) affect the shoreline response. Statistically significant peaks also occur at lower frequencies, associated with cycles typically in the range 2–4 years. We expect that these shoreline motions may well be related to the phenomena discussed in the next section.

3.3. (Inter-)decadal variability

Shoreline variability and mobility on decadal and interdecadal scales of the central Holland coast was investigated by Guillén et al. (1999), using the so-called JARKUS data set over the period 1964–1992. In their analysis they paid particular attention to two regions in which virtually no human interventions took place, so that these could and also appear to develop autonomously, viz. Zones II and III (Fig. 7).

For their analysis, they introduced a profile morphology-based dunefoot position, through which the effect of small-scale profile perturbations could be reduced. The linear trend (through linear regression)

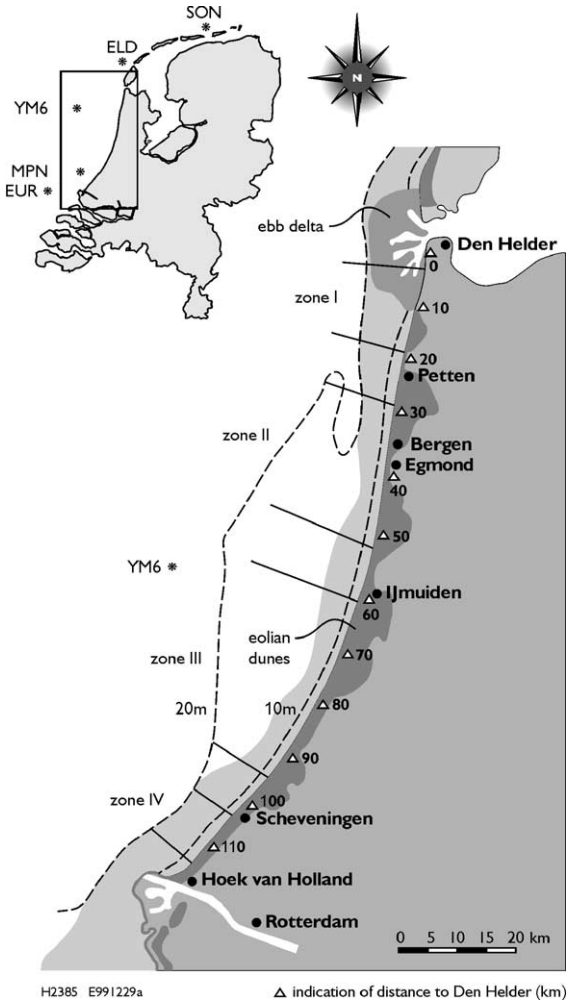

Fig. 7. Location of study area and distinguished zones along the Holland coast, with longshore distances in km measured from Den Helder (adapted from Guillén et al., 1999).

and the standard deviation of this idealised dunefoot show high longshore variability (Fig. 8). Two main regions can be differentiated in the trend of the dunefoot. Northwards of Km 40 erosional trends are dominant and southwards of this location, accretion is dominant. In general, trends are lower than 1 m/year, except in some profiles located close to the harbours. This trend is not considered in the study of Guillén et al. (1999), and it is filtered assuming a linear trend. As treated later on (see section on Holocene Variability), the trend is related to long-term processes, which justifies the assumption of the trend being linear.

The standard deviation of the dunefoot position (or dunefoot mobility) is about 10 m on average and always below 20 m. The standard deviation decreases towards the south from average values of 15 m at Km 10 to 5 m between Km 60 and 90. The mobility of the position of +1 m NAP contour is higher, viz. about 20 m, which may be explained by the fact that dunes are often vegetated, which increases their stability (also cf. Fig. 5a).

Guillén et al. (1999) identified two main factors controlling or forcing the residual dunefoot evolution, i.e., the temporal and spatial variations relative to the trend, along the Holland coast. They concern (1) the influence of subaquaous bar systems (also see Wijnberg, 1995), and (2) variations in the incident cumulative storm-wave energy. Both factors have been found to affect the residual dunefoot evolution of each zone of the coast in a different way.

The influence of the submerged profile in developing alongshore, quasi-rhythmic, patterns has been pointed out in previous studies (Bruun, 1954; Fisher et al., 1984). It is a plausible assumption that bar systems act as a filter for the incident wave energy reaching the beach. Guillén et al. (1999) therefore suggest that the morphological control of the submerged topography on incident wave energy is a dominant factor in developing longshore rhythmic features along the Holland coast. This is in accordance with the observation that the temporal periodicity (about 10–15 years) in the dunefoot fluctuations along Zone II appears to be related to the bar behaviour. A certain cross-shore position of the bar configuration (which displays a return period of 15 years) favours offshore dissipation of incident wave energy and associated shoreline accretion. Other configurations promote wave energy to reach and dissipate on the beach and the shoreline tends to erode. The apparent migration towards the south of the accretional and erosional positions of the dunefoot along Zone II (Fig. 9) is explained by the oblique disposition of bars with respect to the shoreline (cf. Wijnberg and Terwindt, 1995). This results in an apparent alongshore migration of the bar systems and associated rhythmic morphological features, as the bars migrate offshore. In Zone III, bar systems show a more homogeneous displacement and behav-

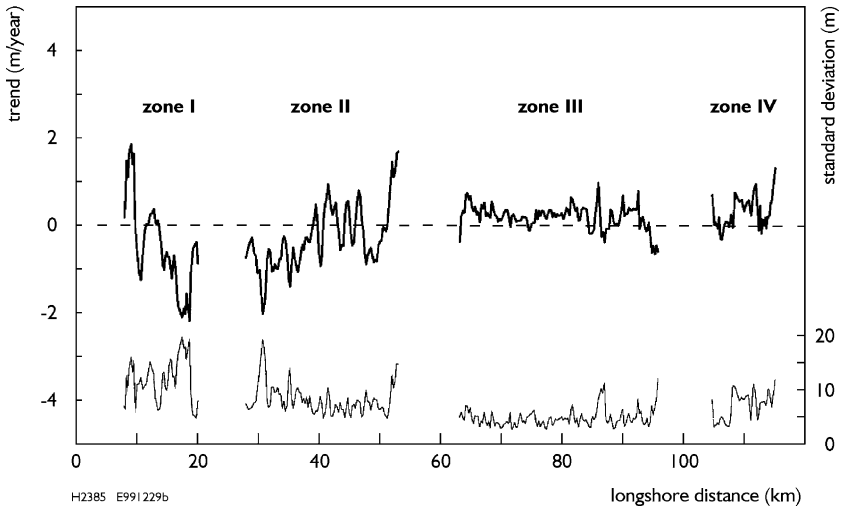

Fig. 8. Linear trend and 'mobility' of the dunefoot position along the Holland coast during the 1964–1992 period (after Guillén et al., 1999).

iour alongshore. The dunefoot evolution is also homogeneous along the coast and no rhythmic patterns are observed. Regional fluctuations in the erosional/accretional positions of the dunefoot simultaneously occur along the entire zone and they seem unrelated to the behaviour of bars. In Zone II the spatially mean temporal fluctuations could be correlated with those of Zone III, indicating that the process responsible for these fluctuations simultaneously affect the entire Holland coast. To illustrate this, Guillén et al. (1999) analysed the wave climate in terms of a cumulative surge-storm parameter and showed that this parameter correlates with fluctuations of the spatially mean shoreline positions of Zones II and III. This suggests that the external forcing by waves and/or storm surges is the responsible mechanism.

Apparently, the behaviour of the nearshore bars is an important controlling factor in the decadal shoreline evolution along the Holland coast. At present, there is no definitive explanation about what processes produce the morphological bar cyclic behaviour, although the change with depth of the relative

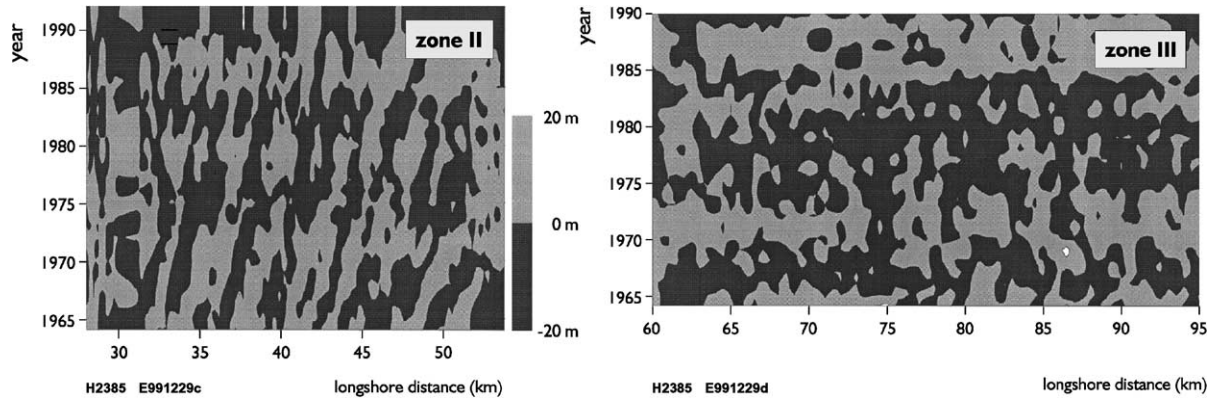

Fig. 9. Residual spatial and temporal variation of dunefoot in Zones II and III; shoreward (dark) and seaward (light). Longshore distances are measured from Den Helder (after Guillén et al., 1999).

importance of bar-degenerating conditions (asymmetric waves) vs. the bar-maintaining conditions (breaking waves) has been proposed as possible mechanism (Wijnberg, 1997). Wijnberg hypothesises that "the exact annual sequence in storm events seems less important for the overall duration of a cycle (of bar evolution) than the fact that a number of varying storm events occurs each year". Guillén et al.'s analysis of storm-wave data along the Holland coast seems to confirm this hypothesis.

3.4. Intercentennial variability due to horizontal or longshore sand waves

The above described spatial and temporal fluctuations in the shoreline for Zone II of the Holland coast belong to a group of phenomena which are called sand waves by Hom-ma and Sonu (1962).[1] The existence of these shoreline fluctuations, with periodicities that are irregular to quasi-sinusoidal in form, is known since Evans (1939). These large-scale (length generally >1 km) crescentic features generally move along the shoreline while maintaining their identity for months to decades, e.g., they move while preserving their form. A summary of sand waves reported on coasts around the world is given in Table 2. The most frequent spatial scales of these rhythmic features are 2–5 km and their rate of migration about 100–300 m (Table 2).

An intriguing question is what cause–effect relationships one is able to identify, which would allow one to assess the reasons for the fluctuations and design appropriate mitigating interventions. Prevailing suggestions are that sand waves are associated with intermittence in sand supply such as the discharge of river sediments, sediments discharged from inlets, artificial injection of a large quantity of sand, and with welding of shoals or oblique bars on to the shore. Two examples are described below, the first related to welded oblique bars, the second related to sediment discharged from a cyclic inlet process.

In a study at Southampton Beach, Long Island, NY, 11 sand waves were identified from aerial photos

[1] Since these features have their amplitude in the horizontal plane, they are generally referred to as 'horizontal sand waves' in the Netherlands. Another suggestion by Thevenot and Kraus (1995) is 'longshore sand waves', emphasizing their longshore dimension.

Table 2
Characteristics of sand waves from literature

Author	Length (km)	Migration rate (m/year)	Amplitude (m)	Period (year)
Bruun (1954)	0.5–3	0–1000	60–80	–
Bakker (1968)	~ 10	150–300	100–400	~ 60
Morton (1979)	5–7	–	–	–
Morton (1979)	2.5–3	–	–	–
Dolan and Hayden (1981)	>1	–	–	–
Stewart and Davidson-Arnott (1988)	0.5–2.5	150–300	50–90	10
Verhagen (1989)[a]	5.5	65	40–60	75–100
Verhagen (1989)[b]	5.5	65	10–20	75–100
Pelczar et al. (1990)	5–9	100–200	70–110	50–60
Thevenot and Kraus (1995)	0.75	350	40	–
Stive et al. (1996)[c]	2–3	150–200	20	15
Arcachon inlet (this paper)	4	100–250	100–400	80

[a] Shoreline data for the Holland coast near coastal inlets.
[b] Shoreline data for the central Holland coast.
[c] Duneface data for the Holland coast.

(Thevenot and Kraus, 1995) along a 15-km-long stretch of coastline. The sand waves had an average length of 0.75 km and an amplitude of about 40 m. Their average migration speed was reported to be 0.35 km/year.

Five sets of aerial photos are available for the 16-month interval from September 1991 to January 1993 at a scale of 1:12,000 and 1:19,200. Fig. 10 shows the locations of the 11 sand waves identified in Thevenot and Kraus (1995) for analysis, giving about one wave per 1.5 km of shoreline. In the figure and the following analysis, only three of the five sets are used. Investigations of associated features showed that the dune line is stationary except when exposed to severe storm waves. Thus, the dunes are not directly impacted by the sand wave location. The subaqueous morphology associated with sand waves appeared as oblique finger shoals, protruding as far as 500 m offshore and pointing in the downdrift direction.

The sand waves were characterised in terms of wave amplitude (a), wavelength (L) and propagation speed (v) from the three sets of photographs. The results are shown in Table 3. The accuracy of the measurements was estimated to about ± 3.5 m, and a

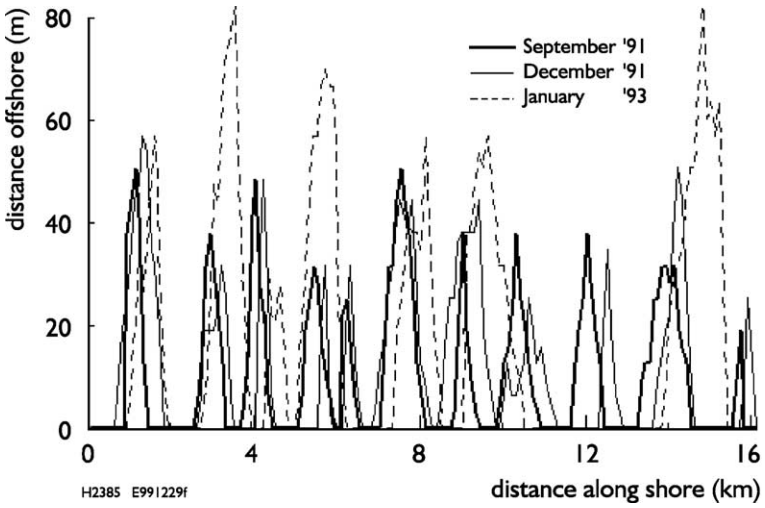

Fig. 10. Measured longshore sandwaves at Southampton Beach, Long Island, NY.

threshold amplitude value of 20 m was applied in the identification. A certain degree of interpretation was required in determining the extent of these features. As seen from the figure and the table, only 7 out of the 11 sand waves are visible in January 1993. The reason for this is believed to be that faster moving sand waves have caught up and merged with slower ones in front of them.

A relatively strong linear relationship ($r=0.84$ at 95% confidence interval) between observed L and v between September 1991 and January 1993 was found, in contrast to Sonu (1968), stating that v would vary inversely with L.

Lorin and Migniot (1984) identified the longest-scale sand waves reported along the Aquitaine Coast (France) in the bay of Biscay by monitoring the position of the dunefoot over 210 km in 1967, 1979, 1982. A rough estimate of the wavelength (about 25 km) and of the celerity (400 m/year) was provided. Due to practical difficulties faced in the field (lack of

Table 3
Amplitude, length, and velocity of longshore sand waves at Southampton Beach, Long Island, NY

SW#	September 1991		9/91–12/91	December 1991		12/91–1/93	January 1993	
	a (m)	L (m)	v (km/year)	a (m)	L (m)	v (km/year)	a (m)	L (m)
1	56	577	0.37	62	812	0.29	62	880
2	42	717	1.32	28	802	0.36	90	1133
3	42	750	0.85	48	425	0.20	28	558
4	35	840	1.32	35	277	0.24	77	1165
5	28	513	0.57	35	398	–	–	–
6	56	1030	1.18	49	1377	0.43	62	1175
7	33	527	1.76	49	1358	0.42	62	1422
8	42	994	1.04	28	1308	–	–	–
9	42	758	2.18	39	530	0.52	69	1528
10	35	1217	0.49	56	940	–	–	–
11	21	285	0.97	28	342	–	–	–
Ave	39	746	1.09	41	779	0.35	64	1130

Positive movement means movement towards west (from Thevenot and Kraus, 1995).

permanent benchmarks, large distance between each measurement section of 3 to 4 km), it was not possible to quantitatively check this variability at the regional scale.

On the other hand, locally, more data was available around the Arcachon inlet located in the centre of the Aquitaine Coast. Thanks to precise bathymetric surveys, available since 1826, the cyclic behaviour of the inlet (period of about 80 years) was established (Orgeron, 1974) and further described by Michel and Howa (1997). This cyclic behaviour is visualised in Fig. 11a to f, providing the position of the channels between 1826 and 1988. Very similar positions are observed between the 1826 (Fig. 11a), 1905 (Fig. 11b), and 1988 (Fig. 11f) surveys.

This cycle is driven by the littoral drift estimated at 0.63 millions m^3/year on average from north to south. As a result, sand is accumulated at Cape Ferret in the North, creating a sand bank which at a certain moment starts to cross the inlet and impacts the southern shore in the south of dune de Pilat. Such an impact was recorded by aerial photographs in 1959 (Fig. 12a) and the movement of the created sand waves monitored by aerial photographs of 1964, 1973, 1984, 1991, and 1996 (see Fig. 12b to f).

A decay of the sand waves amplitude is clearly observed and the celerity of the front is estimated between 100 to 250 m/year (length of about 4 km). Michel et al. (1995) have surveyed the low water line of the bank every month between September 1991 and April 1993 and show an experimental decay of the wave amplitude. Bakker (1968) has observed a similar exponential decay, for a very similar situation on one of the Wadden islands.

3.5. Intercentennial variability due to climate change

There seems to exist some evidence that on intercentennial scales natural, spatially uniform shoreline changes may occur due to temporary changes or fluctuations in the regional meteorological climate and/or wave climate. An example of this is the correlation that Van Straaten (1961) found between the temporary changes in the demeaned position of the Holland coast shoreline and those in the meteorological conditions during 1855 and 1900 (Fig. 13). During this period, Northwestern winds decreased some 3% relative to the long-term trend, while Southwestern and Western winds increased some 3% to 4%. This specific change in the windclimate coincided with a shore retreat of the LW shoreline (relative to the long-term trend) of 20 to 100 m, which has been observed generally over the Holland coast. The phase difference between meteorological changes and shoreline changes is approximately 5 years (cf. Fig. 13). It is noted that these changes have been observed in the HW and LW shoreline, but have not been observed in the position of dunefoot.

Although the above correlation seems quite clear, it has never been satisfactorily proven that the implied cause–effect relationship is true. Other suggestions (Stolk, 1989) are that the phenomenon coincides with a temporary lowering of mean sea level from approximately 1880 to 1900, which can also explain a temporary progradation. As we have discussed earlier, similar correlations between ‘wave’ climate change/variation and spatially uniform shoreline response are found on smaller time scales. This would then support the suggestions of Van Straaten (1961).

3.6. Late Holocene (millennial) variability

Based on observations of large-scale Holocene coastal behaviour, Cowell et al. (2002) consider a ‘‘coastal tract’’ system to form the lowest or first-order level in a hierarchy of coastal evolution scales. On larger time scales (centuries to millenia) a coastal tract extends over a significant portion of the periphery of the shelf. It may include, for instance, deltas, shorefaces, dunes, and (tidal) lagoons, and responds in a morphologically coupled sense to higher level-related forcing conditions, such as relative sea-level rise and shelf-controlled hydrodynamic conditions, and to lower level constraints, such as a geologically inherited substrate (the zero-order system). On these larger time scales, the coastal tract is a sediment sharing, dynamically transient system. Within the tract, sediment is conserved, taking into account

Fig. 11. Evolution of the Arcachon tidal inlet (France): shoreline and isobath (− 5.0 m). (a) 1826; (b) 1905 (includes installment years of lighthouses); (c) 1938; (d) 1948; (e) 1972; (f) 1988.

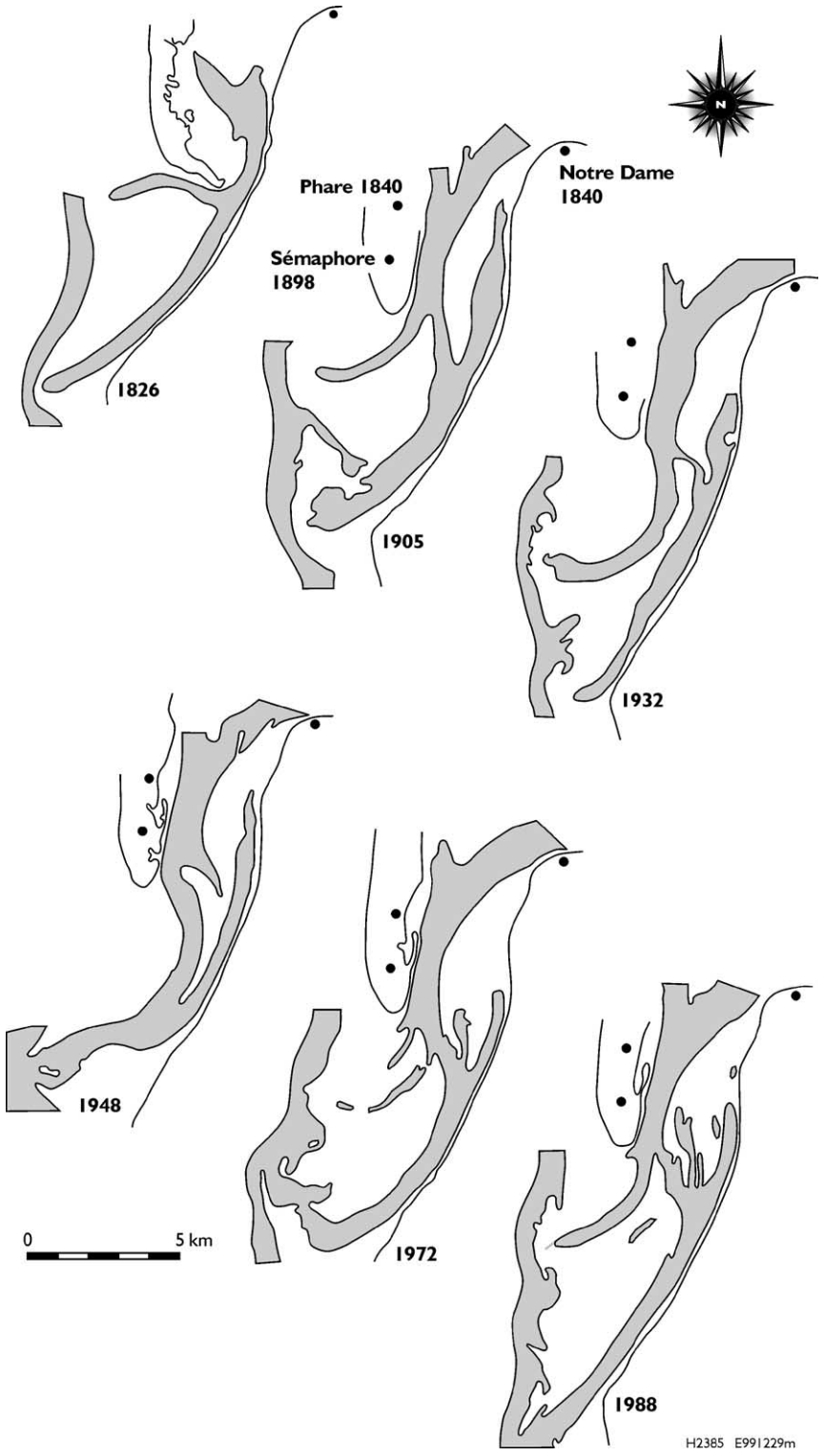
Phare 1840
Notre Dame
1840
Sémaphore
1898
1826
1905
1932
1948
1972
1988
0
5 km
H2385 E991229m

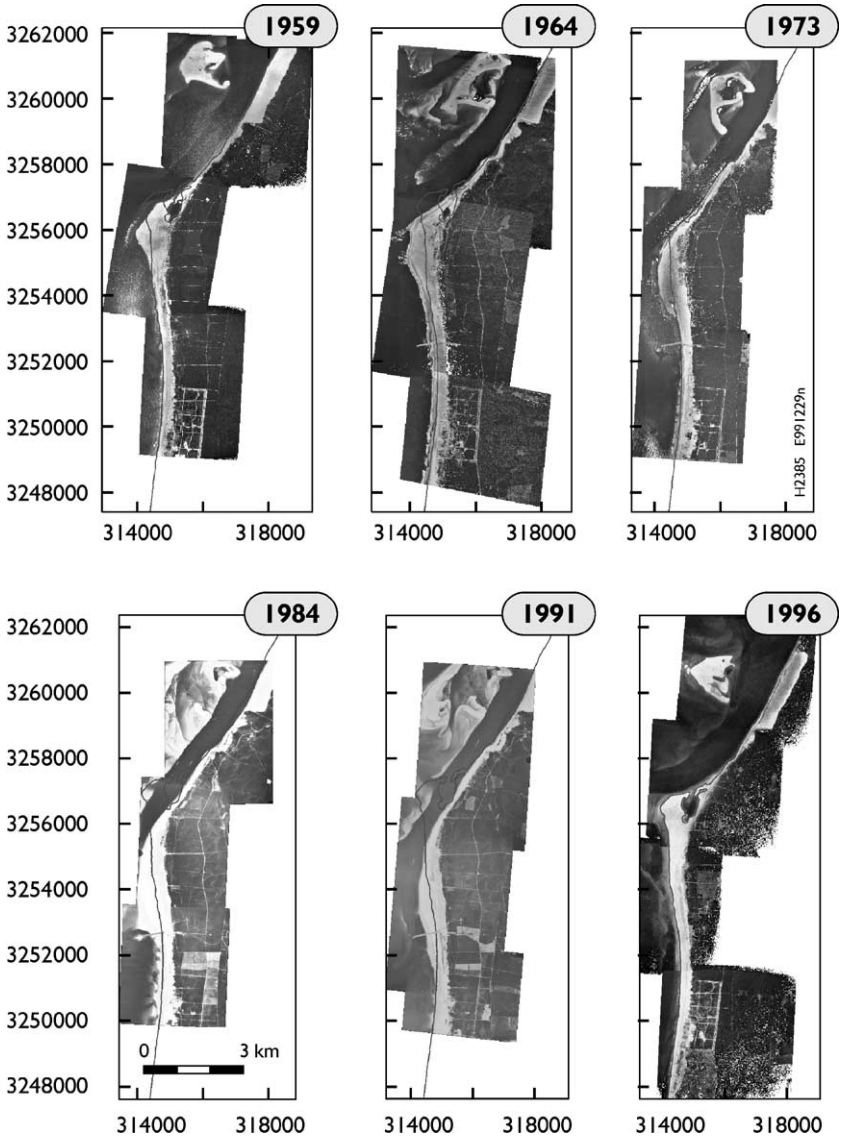

Fig. 12. Evolution of a sand wave in the southern part of the Arcachon inlet (original aerial photographs from Institut Géographique National, France). (a) 1959; (b) 1964; (c) 1973; (d) 1984; (e) 1991; (f) 1996.

external sediment sources (such as river input) or sinks (such as submarine canyons) and internal effects which remove or add sediment (such as subsidence or uplift, or biogenic sediment production or solution).

In order to deal with the complexity of a coastal tract system, there is a need to further partition the system. They therefore introduce a higher, second-order level at which they attempt to describe the spatial and functional complexity of the coastal tract system. This may be referred to as the level of 'physiographic units'. Examples of the coastal physiographic units we may distinguish are a river delta, an inlet-free shoreface, a beach barrier, a coastal inlet, or a backbarrier system (lagoon, bay or estuary).

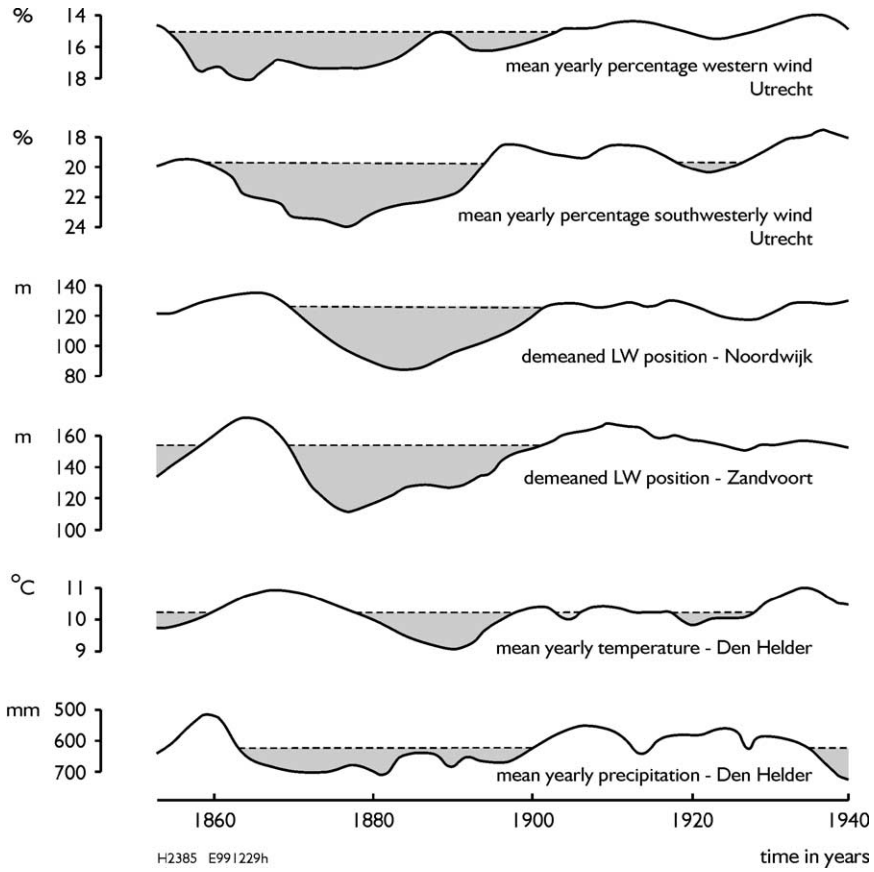

Fig. 13. Correlation between meteorological conditions and the demeaned shoreline position from 1848 to 1944 (adapted after Klijn, 1981 and Van Straaten, 1961).

The evolution of the Holland coastal tract over the Late Holocene is here introduced to describe the potential variability in the shoreline trend over time of an approximately 100-km-long shoreface stretch under a variable rate of sea-level rise and sediment availability.

From approximately 5000–2000 BP (i.e., years Before Present), the first-order "sediment sharing" system concerns the central Holland coastal tract flanked by the Rhine Meuse Delta in the South and the Texel High in the North (Fig. 14). Both the Delta and the High are assumed to have an alongshore sediment divergence point in the transport at their inferred location of maximum protrusion. Before 5000 BP, the Pleistocene depression between the Rhine Meuse Delta and the Texel High was a sheltered tidal basin- or lagoon-like area in which during strong sea-level rise the sea transgressed and marine sedimentation occurred. Several larger inlets developed which stored sediments in their ebb and flood tidal deltas. As sea level rises, rates started to drop the lagoon inlets choked, and a strongly prograding barrier system came into being, storing some 6 billion m^3 of sediments between 5000 and 2000 BP (Beets et al., 1992). It is estimated that somewhat less than half of this amount was laterally fed by the Rhine Meuse Delta and to a lesser extent by the Texel High. The remainder is estimated to have been reworked from the shoreface, primarily from the subaquaous tidal deltas and secondarily from the deeper shoreface. Since 2000 BP, the role of the delta as a southern source, although decreasing in magnitude, has not basically changed. The Texel High, however, started to loose its integrity by breakthroughs and washovers, and instead

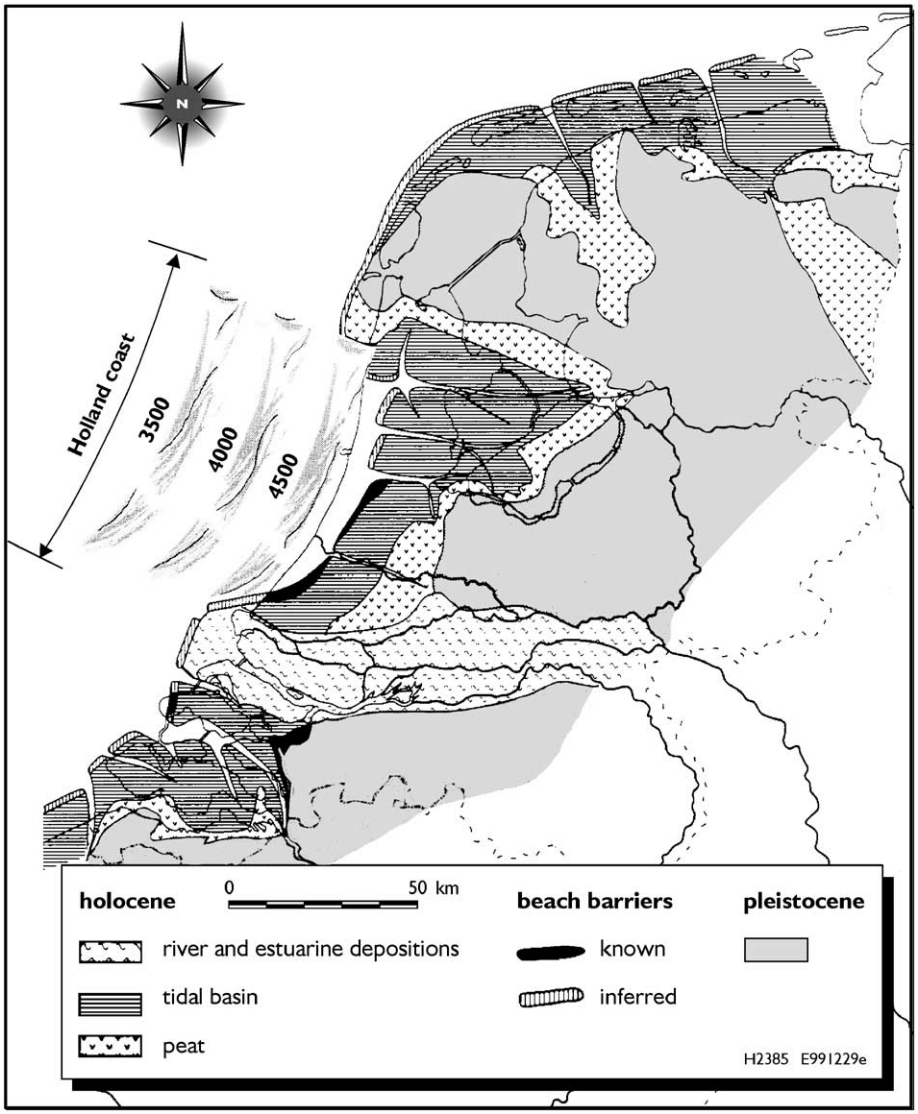

Fig. 14. Reconstruction of the first-order sediment sharing system of the Holland coastal tract (approximately 6000 BP). Inset: Isochrons of the Holland Coast barrier sequence in years BP (after Beets et al., 1992).

of being a source towards the south, it developed into a source for the Wadden Sea barrier islands and tidal basins.

More detailed quantitative data on the resulting shore position evolutions over the period 5000 BP until present has been derived on the basis of geological and historical reconstructions, supported by modelling. These have been collected in the framework of the Coastal Genesis project (Stive, 1987) and presented, reviewed, and analysed in the context of the studies underbuilding the formulation of the Netherlands Coastal Defence Strategy of 1990 (Stive and Eysink, 1989). Below these data are summarised for the specific purpose of isolating the role of direct (the Bruun effect) effects of sea-level rise from a collection of other process effects, such as indirect effects of sea-level rise and effects due to cross-shore and longshore gradients (Stive et al., 1990). In doing

so, we distinguish three second-order systems over the Late Holocene along the Holland coastal tract (Fig. 14).

3.6.1. Scheveningen–Bergen transect between 5000 and 2000 BP (Zones II and III, Fig. 7)

The barrier system between Scheveningen and Bergen (some 75 km in length) can be considered as a subsystem of the above first-order system. As illustrated by a number of isochrons of this barrier sequence (Beets et al., 1992)), we are dealing here with a rather uniform prograding shoreface between 5000 and 2000 BP. Shoreline evolution and sea-level rise rates for this transect are given in Table 4a. The sediment sources for this system appear to be far greater than the sinks due to sea-level rise and possibly dune formation.

Based on the method of Cowell et al. (2002), an estimate of the contribution of sea-level rise to shoreline movement in the cross-shore direction (the 'direct' effect of sea-level rise) can be made. The method uses the concept that the sediment budget and the resulting shoreline evolution are determined by (1) the assumption that the morphologically active part of the shoreface remains invariant relative to mean sea level (the Bruun effect), and (2) the remaining external and internal sources. This yields an absolute, i.e., compared to the gross contributions of all effects when each effect is taken absolute, contribution of the sea-level rise component of less than 5%.

3.6.2. Hoek of Holland–Haarlem transect between 2000 BP and present (Zone III, Fig. 7)

The southern part of the original Scheveningen–Bergen transect, although not being fed as strongly by the delta, initially continued its advance. At a later stage, it experienced strong cross-shore redistribution by the formation of the Younger dunes (AD ~ 1000 to 1650), and shore retreat occurred. Supported by dune management and since the construction of the harbours of Rotterdam and IJmuiden (after AD 1850), the upper shoreface of this transect is accretive (also see Fig. 8). The sources are decreasing net longshore transport from the south and erosion of the lower shoreface, compensating for the sinks due to sea-level rise and dune formation. Table 4b gives an estimate of the average shoreline evolution and associated sea-level rise rates over the various periods.

The estimate of the contribution of sea-level rise to the shoreline movement yields an absolute contribution of this component of 10% for the period AD 0–1000, 4% for the period AD 1000–1500, 7% for the period AD 1500–1850, and 17% for the period of 1850 to present.

3.6.3. Haarlem–Den Helder transect between 2000 BP and present (Zone II, Fig. 7)

As indicated above, the northern part of the original Scheveningen–Bergen transect and the adjacent Texel High started to play a role as sediment source for the North-Holland breakthroughs and the adjacent Wadden Sea system. These sediment losses were

Table 4a
Data for Scheveningen–Bergen transect between 5000 and 2000 BP

Period		Sea-level rise rate	Shoreline evolution
C^{14} years BP	Calendar years		
~ 5000–4000 BP	~ 4000–2700 BC	~ 2 mm/year	~ 2.1 m advance/year
~ 4000–2000 BP	~ 2700 BC–AD 0	~ 1 mm/year	~ 1.6 m advance/year

Table 4b
Data for Hoek of Holland–Haarlem transect between 2000 BP and present

Period	Sea-level rise rate	Shoreline evolution
Calendar years		
AD ~ 0–1000	0.5–1 mm/year	~ 0.3 m advance/year
AD ~ 1000–1500	0.5–1 mm/year	~ 1.1 m retreat/year
AD ~ 1500–1850	0.5–1 mm/year	~ 0.6 m retreat/year
AD ~ 1850–present	1.5–2 mm/year	~ 0.45 m advance/year

Table 4c
Data for Haarlem–Den Helder transect between 2000 BP and present

Period	Sea-level rise rate	Shoreline evolution
Calendar years		
AD ~ 0–1000	0.5–1 mm/year	~ 1.7 m retreat/year
AD ~ 1000–1500	0.5–1 mm/year	~ 3.9 m retreat/year
AD ~ 1500–1850	0.5–1 mm/year	~ 2.7 m retreat/year
AD ~ 1850–present	1.5–2 mm/year	~ 1.65 m retreat/year

aggravated by the formation of the Younger dunes resulting in strong retreat, which persists until present (see also Fig. 8). Table 4c gives an estimate of an average shoreline evolution and associated sea-level rise rates over the various periods.

Here, the estimate of the 'direct' contribution of sea-level rise to shoreline movement yields an absolute contribution of this component of less than 5% in all cases. However, as highlighted by Stive et al. (1990), there exists an 'indirect' impact of sea-level rise due to the sediment accommodation space created by this rise in the adjacent Wadden Sea tidal basin. This component has become dominant in recent times due to growth of the Wadden Sea and the small, but significant, increase in relative sea-level rise.

The above example is introduced to give an insight into the controls on long-term shoreline trends and their variations on centennial scales, against the background of sea-level rise rates. Important lessons are that the 'direct' effect of sea-level rise (known as the Bruun effect; Bruun, 1962) is fairly modest under rates of Late Holocene sea-level rise (as occurring in stable areas), and that the importance of lateral sources and sinks is high and dominated by the 'indirect' effect of sea-level rise when the coast is under the influence of an adjacent tidal basin. It is finally stressed though that for lateral sources and/or sinks for an inlet-free shoreline to exist requires that either the coast displays a curvature relative to the offshore wave climate or that there exist protrusions such as due to a delta.

4. Discussion and conclusions

We have presented and discussed a broad variety of time and space scales of natural and human-induced causes or factors (forcing or input) and the resulting shoreline evolution (response or output). While the forcing at all scales can consist of natural forcing (delivered by the larger scales) and human forcing (theoretically at all scales), it is typically at decadal and centennial scales (years to hundreds of years) that important human-induced forcing is exerted. We find that at these scales, the shoreline and the shore can exhibit spatially and temporally uniform and spatially and temporally fluctuating motions of significant magnitude. Importantly, these fluctuating motions can be larger than the uniform centennial and decadal motions and the structural longer-term (millennial) trends such as discussed for the Holland coast. Therefore, these fluctuations need to be considered to fully understand shoreline evolution, in general, and to properly design shore nourishment interventions, in particular. Since it may be expected that the intervention scales are of a similar magnitude to the fluctuating motions, scale interactions may occur leading to unforeseen evolution (Capobianco et al., 2002). If we understand the reasons behind centennial and decadal variability, we may design shore nourishments such that human interventions work in concert with natural processes rather than in conflict (Hamm et al., 2002). This should minimise the magnitude and long-term cost of such human interventions in the coastal system.

This latter argument also holds for larger-scale variability. If, for example, we are able to attribute a significant part of a structural (long-term) erosion trend to sediment demand of an adjacent tidal basin, one may decide to nourish the sediment sharing system at a more efficient and effective location, e.g., at the ebb-tidal delta, so as to feed the sink more directly (and at a lower cost).

At smaller scales, seasonal and annual variability should also be taken into account when designing shore nourishments. In principle, if the nourishment source material does not differ too much from the native material, we may expect that the natural variability to remains approximately constant. However, this variability has elements of unpredictability, amongst other factors because of the stochastic nature of the hydrodynamic climate. Understanding such probabilistic behaviour requires more attention than it has received so far (Capobianco, 1998).

We have provided an insight into shore variability based on observations, accompanied by a description of possible causes and factors for the variability. Although there appear to be some interesting qualitative insights into the reasons behind shore variability, it is difficult to derive quantitative, generic information for arbitrary situations, mainly because we presently have insufficient quantitative physical insight. One way to further our understanding of shore variability is a system approach that explores the transfer function between system input and system output, which is determined by the properties of the coastal

dynamics behaviour (the system). However, complicating such an approach to analysis, it is increasingly recognised that the coastal system's response may comprise both *forced* behaviour and *free* behaviour (Dodd et al., 2002). At centennial and decadal scales, we have little insight into the possible free behaviour. Rather, there is the common temptation to aggregate our input and system's behaviour such that we are left with forced behaviour only: deviations due to free behaviour are either calibrated out or encapsulated in the margins of prediction accuracy.

At smaller time and space scales, we are both starting to explore free behaviour (Dodd et al., 2002) and capturing the limits of deterministic predictability (Capobianco, 1998). For these scales, we would want to emphasise the importance of research into the chronology of the input and the importance of high-resolution observations of the output using remote-sensing techniques such as the ARGUS video technique. However, at decadal and larger scales, we are only beginning to explore methodologies to assess the impacts of forcing. As this paper has shown, this is a valuable exercise that deserves further attention as it will lead to important and useful insights into input-forced coastal evolution.

Acknowledgements

These results are largely based on work in the SAFE project, in the framework of the EU-sponsored Marine Science and Technology Programme (MAST-III), under contract no. MAS3-CT95-0004.

The various authors have received matching funds from national research programmes. MJFS was partly funded by the Netherlands Centre for Coastal Research and the Delft Cluster Project Coasts DC-03.01.03. SJCA was partly funded by the DIOC-Earth Observation Project of Delft University of Technology. LH received additional funding from Ministère de l'Equipement, des Transports et du Logement, Direction de la Recherche et des Affaires Scientifiques et Techniques, Service Technique des Ports Maritimes et des Voies Navigables (France), subvention no. 97M/3. HH and ML were partly funded by the Swedish Natural Science Research Council. KW received additional support from the ONR NICOP programme. RJN received funding from PACE under contract no. MAS3-CT95-002 (a sister project to SAFE).

Valuable, partly unpublished, data were provided by several researchers, which is gratefully acknowledged. The video data of Florida is courtesy of Dr. Abe Sallenger, USGS, St. Petersburg, FL, USA. The shoreline data of North Carolina is courtesy of Dr. Jeff List, USGS, Woods Hole, USA. The data from Ogata beach is courtesy of Dr. Takao Yamashita, Disaster Prevention Research Institute, Kyoto University, Japan. The cooperation of the staff at the Field Research Facility and its Chief Mr. William Birkemeier in providing Duck profile data used in parts of this work is greatly appreciated.

The manuscript significantly improved on the basis of the review comments by Dr. Jeff List.

References

Bakker, W.T., 1968. A mathematical theory about sand waves and its application on the Dutch Wadden Isle of Vlieland. Shore Beach 36 (2), 4–14.

Beets, D.J., van der Valk, L., Stive, M.J.F., 1992. Holocene evolution of the coast of Holland. Mar. Geol. 103, 423–443.

Birkemeier, W.A., Nicholls, R.J., Lee, G., 1999. Storm groups and morphologic change in the nearshore. Proceedings Coastal Sediments 99. ASCE, New York, pp. 1109–1122.

Bruun, P., 1954. Migrating sand waves or sand humps, with special reference to investigations carried out on the Danish North Sea Coast. Proc. 5th Int. Conf. Coast. Eng. ASCE, New York, pp. 269–295.

Bruun, P., 1962. Sea-level rise as a cause of shore erosion. ASCE J. Waterw. Harb. Div. 88 (WW1), 117–130.

Capobianco, M., 1998. Predictability for long-term coastal evolution—handling the limiting factors. 3rd European Marine Science and Technology Conference, Scientific Colloquium Predictability for Long-term Coastal Evolution—Is it Feasible? 23–27 May, Lisbon, Portugal, 277–288.

Capobianco, M., Stive, M.J.F., Jiménez, J.A., Sanchez-Arcilla, A., 1998. Towards the definition of budget models for the evolution of deltas. J. Coast. Conserv. 4, 7–16.

Capobianco, M., Hanson, H., Larson, M., Steetzel, H.J., Stive, M.J.F., Chatelus, Y., Hamm, L., Aarninkhof, S., Karambas, T., 2002. Nourishment design and evaluation: applicability of model concepts. Coast. Eng. 47, 113–135.

Cowell, P.J., Stive, M.J.F., Niedoroda, A.W., De Vriend, H.J., Swift, D.J.P., Kaminsky, G.M., Capobianco, M., 2002. The coastal-tract (Part 1): a conceptual approach to aggregated modelling of low-order coastal change. Spec. Issue J. Coast. Res. (in press).

Dettinger, M.D., Ghil, M., Strong, C.M., Weibel, W., Yiou, P., 1995. Software expedites singular-spectrum analysis of noisy

time series. EOS, Transactions American Geophysical Union 76 (2), p. 12, 14, 21.

Dodd, N., Blondeaux, P., Calvete, D., De Swart, H.E., Falques, A., Hulscher, S.J.M.H., Rózynski, G., Vittori, G., 2002. The use of stability methods for understanding the morphodynamical behavior of coastal systems. Spec. Issue J. Coast. Res. (in press).

Dolan, R., Hayden, B.P., 1981. Storms and shoreline configuration. J. Sediment. Petrol. 51, 737–744.

Dolan, R., Hayden, B.P., Heywood, J., 1978. Analysis of coastal erosion and storm surge hazards. Coast. Eng. 2, 41–53.

Evans, O.F., 1939. Mass transport of sediments on subaqueous terraces. J. Geol. 47, 324–334.

Fisher, N., Dolan, R., Hayden, B.P., 1984. Variations in large-scale beach amplitude along the coast. J. Sediment. Petrol. 54 (1), 73–85.

Guillén, J., Stive, M.J.F., Capobianco, M., 1999. Shoreline evolution of the Holland coast on a decadal scale. Earth Surf. Processes Landf. 24, 517–536.

Hamm, L., Capobianco, M., Dette, H.H., Lechuga, A., Spanhoff, R., Stive, M.J.F., 2002. A summary of European experience with shore nourishment. Coast. Eng. 47, 237–264.

Hom-ma, M., Sonu, C., 1962. Rhythmic patterns of longshore bars related to sediment characteristics. Proc. 8th Coast. Eng. Conf. ASCE, New York, pp. 248–278.

Howd, P.A., Birkemeier, W.A., 1987. Beach and nearshore survey data: 1984–1984 CERC Field Research Facility. Technical Report CERC-87-9, Coastal Engineering Research Center, US Army Engineer Waterways Experiment Station, Vicksburg, MS.

Klijn, J.A., 1981. Coastal Dunes of The Netherlands: Geomorphology and Bottom (in Dutch). PUDOC, Wageningen. 188 pp.

Komar, P., 1998. Beach and Nearshore Sedimentation, 2nd ed. Prentice-Hall, Upper Saddle River, NJ, USA.

Lee, G., Birkemeier, W.A., 1993. Beach and nearshore survey data: 1985–1991 CERC Field Research Facility. Technical Report CERC-93-3, Coastal Engineering Research Center, US Army Engineer Waterways Experiment Station, Vicksburg, MS.

Lippmann, T.C., Holman, R.A., 1990. The spatial and temporal variability of sand bar morphology. J. Geophys. Res. 95 (C7), 11575–11590.

List, J.H., Farris, A.S., 1999. Large-scale shoreline response to storms and fair weather. Proc. Coastal Sediments '99. ASCE, Reston, VA, pp. 1324–1338.

Lorin, J., Migniot, C., 1984. Recul du trait de côte le long du littoral aquitain. Notion de sédimentologie prévisionnelle. Proc. 18ème journées de l'hydraulique, 11–13 Septembre 1984, Marseille, France. Société Hydrotechnique de France, Paris, France, pp. 11.6.1–11.6.9.

Masselink, G., Short, A.D., 1993. The effect of tide range on beach morphodynamics and morphology: a conceptual model. J. Coast. Res. 9 (3), 785–800.

Michel, D., Howa, H., 1997. Morphodynamic behaviour of a tidal inlet system in a mixed-energy environment. Phys. Chem. Earth 22 (3–4), 339–343.

Michel, D., Howa, H., Tastet, J.P., 1995. Modelling of the morphological evolution of an intertidal sand bank (south of the Arcachon lagoon, France). C. R. Acad. Sci. Paris 321 (IIa), 497–504.

Morton, R.A., 1979. Temporal and spatial variations in shoreline changes and their implications, examples from the Texas Gulf Coast. J. Sediment. Petrol. 49, 1101–1111.

Moulis, D., Loubié, S., Heurtefeux, H., 1999. Spit of the Gracieuse (France). Data report. Internal report Institut des Aménagements Régionaux et de l'environnement, SAFE project.

Orgeron, C., 1974. Sédimentologie des passes d'entrée du bassin d'Arcachon. Bull. Inst. Geol. Bassin Aquitaine 15, 31–51.

Pelczar, M., Nejczew, P., Mielczarski, A., 1990. Cartometric analysis of the shore-line changes on eastern part of the Polish Baltic coast in the last century (in Polish). Rozpr. Hydrotech. 51.

Plant, N.G., Holman, R.A., 1997. Intertidal beach profile estimation using video images. Mar. Geol. 140, 1–24.

Rózynski, G., Larson, M., Pruszak, Z., 2001. Forced and self-organized shoreline response for a beach in the southern Baltic Sea determined through singular spectrum analysis (SSA). Coast. Eng. 43 (1), 41–58.

Short, A.D., Hesp, P., 1982. Wave, beach and dune interaction in southeastern Australia. Mar. Geol. 48, 259–284.

Sonu, C.J., 1968. Collective movement of sediment in littoral environment. Proc. 11th Coastal Eng. Conf. ASCE, pp. 373–398.

Southgate, H.N., Wijnberg, K.M., Larson, M., Capobianco, M., Jansen, H., 2002. Analysis of field data of coastal morphological evolution over yearly and decadal timescales: Part 2. Non-linear techniques. J. Coast. Res. (Special Issue, in press).

Stewart, C.J., Davidson-Arnott, R.G.D., 1988. Morphology, formation and migration of longshore sandwaves; Long Point, Lake Erie, Canada. Mar. Geol. 81, 63–77.

Stive, M.J.F., 1987. Coastal Genesis Main Report, Phase 1 (in Dutch), September 1987. 87 pp.

Stive, M.J.F., Eysink, W.D., 1989. Coastline Prediction 1990–2090. Report 3.1: Dynamic model of the Netherlands Coastal System (in Dutch). WL | Delft Hydraulics Report M 825-IV, 117 pp.

Stive, M.J.F., Roelvink, J.A., De Vriend, H.J., 1990. Large-scale coastal evolution concept. The Dutch Coast. Proc. 22nd Int. Conf. Coast. Eng., vol. 9. ASCE, New York, pp. 1962–1974.

Stive, M.J.F., Guillén, J., Capobianco, M., 1996. Bar migration and duneface oscillation on decadal scales. Proc. 25th Int. Conf. Coast. Eng. ASCE, New York, pp. 2884–2896.

Stolk, A., 1989. "Sand system coast—a morphological characterisation—coastal defence after 1990" (in Dutch). Report GEOPRO 1989.02, p. 97.

Thevenot, M.M., Kraus, N.C., 1995. Longshore sandwaves at Southampton Beach, New York: observation and numerical simulation of their movement. Mar. Geol. 126, 249–269.

Thomson, D.J., 1982. Spectrum estimation and harmonic analysis. Proc. IEEE 70, 1055–1056.

Tsuchiya, Y., Yamashita, T., Izumi, T., 1994. Erosion control by considering large scale coastal behavior. Proc. 24th Int. Coast. Eng. Conf. ASCE, New York, pp. 3378–3392.

Uda, T., Ito, H., Saito, T., 1990. Summarized data of beach profiles and wave observations at Ajigaura Beach (2). Technical Memorandum of PWRI No. 2900, Coastal Engineering Division, River Department, Public Works Research Institute, Ministry of Construction, Tsukuba, Japan.

Van Straaten, L.M.J.U., 1961. Directional effects of winds, waves

and currents along the Dutch North Sea coast. Geologie en Mijnbouw, 40, 333–346 (Part 1) and 363–391 (Part 2).

Vautard, R., Yiou, P., Ghil, M., 1992. Singular spectrum analysis: a toolkit for short, noisy chaotic signals. Physica D 58, 95–126.

Verhagen, H.J., 1989. Sand waves along the Dutch coast. Coast. Eng. 13, 129–147.

Wijnberg, K.M., 1995. Morphologic behaviour of a barred coast over a period of decades. PhD thesis, University of Utrecht, p. 250.

Wijnberg, K.M., 1997. On the systematic offshore decay of breaker bars. Proc. 25th Int. Conf. Coast. Eng. ASCE, New York, pp. 3600–3613.

Wijnberg, K.M., Terwindt, J.H.J., 1995. Extracting decadal morphological behaviour from high-resolution, long-term bathymetric surveys along the Holland coast using eigenfunction analysis. Mar. Geol. 126, 301–330.

Wright, L.D., Short, A.D., 1984. Morphodynamic variability of surf zones and beaches: a synthesis. Mar. Geol. 56, 93–118.

Wright, L.D., Short, A.D., Green, M.O., 1986. Short-term changes in the morphodynamic states of beaches and surf zones: an empirical predictive model. Mar. Geol. 62, 339–364.